Chapter 4
Bayesian Uncertainty Quantification and Propagation in Nonlinear Structural Dynamics

Dimitrios Giagopoulos, Dimitra-Christina Papadioti, Costas Papadimitriou, and Sotirios Natsiavas

Abstract A Bayesian uncertainty quantification and propagation (UQ&P) framework is presented for identifying nonlinear models of dynamic systems using vibration measurements of their components. The measurements are taken to be either response time histories or frequency response functions of linear and nonlinear components of the system. For such nonlinear models, stochastic simulation algorithms are suitable Bayesian tools to be used for identifying system and uncertainty models as well as perform robust prediction analyses. The UQ&P framework is applied to a small scale experimental model of a vehicle with nonlinear wheel and suspension components. Uncertainty models of the nonlinear wheel and suspension components are identified using the experimentally obtained response spectra for each of the components tested separately. These uncertainties, integrated with uncertainties in the body of the experimental vehicle, are propagated to estimate the uncertainties of output quantities of interest for the combined wheel-suspension-frame system. The computational challenges are outlined and the effectiveness of the Bayesian UQ&P framework on the specific example structure is demonstrated.

Keywords System identification • Uncertainty identification • Bayesian inference • Nonlinear dynamics • Substructuring

4.1 Introduction

Structural model updating methods (e.g. [1]) are used to reconcile linear and nonlinear mathematical models of a mechanical system with available experimental data from component or system tests. For complex structural dynamics models it is often the case that these models are usually discretized linear finite element (FE) models for a large part of the structure with localized nonlinearities in isolated structural parts. Examples include vehicle models that consist of linear structural components, such as the body of the vehicle, and nonlinear structural components, such as the suspension and the wheel components, which may exhibit strongly nonlinear behaviour. To build high fidelity models for such complex structures with localized nonlinearities, one should reconcile linear and nonlinear structural models with experimental data available at both the component and system level. This work presents the challenges of Bayesian uncertainty quantification and propagation of complex nonlinear structural dynamics models and results of identification of nonlinear models of a small scale experimental vehicle consisting of linear and nonlinear components. The goal is to build high fidelity models of the components to simulate the behaviour of the combined system.

Bayesian techniques [2, 3] have been proposed to quantify the uncertainty in the parameters of a structural model, select the best model class from a family of competitive model classes [4, 5], as well as propagate uncertainties for robust response

D. Giagopoulos
Department of Mechanical Engineering, University of Western Macedonia, Kozani, Greece
e-mail: dgiagopoulos@uowm.gr

D.-C. Papadioti · C. Papadimitriou
Department of Mechanical Engineering, University of Thessaly, Volos, Greece
e-mail: costasp@uth.gr; dxpapadioti@uth.gr

S. Natsiavas (✉)
Department of Mechanical Engineering, Aristotle University, Thessaloniki, Greece
e-mail: natsiava@auth.gr

T. Simmermacher et al. (eds.), *Topics in Model Validation and Uncertainty Quantification, Volume 5*,
Conference Proceedings of the Society for Experimental Mechanics Series 41,
DOI 10.1007/978-1-4614-6564-5_4,

and reliability predictions [6]. Posterior probability density functions (PDFs) are derived that quantify the uncertainty in the model parameters based on the data. For nonlinear structural models, the measurements are taken to be either response time histories or frequency response functions of nonlinear systems. Computationally intensive stochastic simulation algorithms (e.g., Transitional MCMC [7]) are suitable tools for identifying system and uncertainty models as well as for performing robust prediction analyses. These algorithms require a large number of system analyses to be performed over the space of uncertain parameters. However, for relatively large order FE models involving hundreds of thousands or even million degrees of freedom and localized nonlinear actions activated during system operation, such re-analyses may require excessive computational time. Methods for drastically reducing the computational demands at the system, algorithm and hardware levels involved in the implementation of Bayesian framework have recently been developed. At the system level, efficient computing techniques can be integrated with the Bayesian framework to handle large order models and localized nonlinear action. Specifically, component mode synthesis and multilevel substructuring techniques can achieve substantial reductions in computational effort.

At the system level, efficient computing techniques are integrated with Bayesian techniques to efficiently handle large order models of hundreds of thousands or millions degrees of freedom (DOF) and localized nonlinear actions activated during system operation. Specifically, fast and accurate component mode synthesis (CMS) techniques have recently been proposed [8], consistent with the FE model parameterization, to achieve drastic reductions in computational effort. In addition, automated multilevel substructuring techniques [9] are used to achieve substantial reductions in computational effort in the re-analysis of linear substructures. At the level of the Transitional MCMC (TMCMC) algorithm, surrogate models are adopted to drastically reduce the number of computationally expensive full model runs [10]. At the computer hardware level, parallel computing algorithms are proposed to efficiently distribute the computations in available multi-core CPUs [10].

In this work the Bayesian UQ&P framework is applied to identify models of linear and nonlinear components of a small scale experimental model of a vehicle. The identification of the uncertainty models of the nonlinear wheel and suspension components is investigated using the experimentally obtained response spectra. The uncertainty models for the vehicle frame are also obtained using experimental data. The uncertainty is propagated to output quantities of interest for the combined wheel-suspension-frame system. The computational challenges and efficiency of the Bayesian UQ&P framework are outlined. The effectiveness of the framework on the specific example structure is discussed.

4.2 Review of Bayesian Formulation for Parameter Estimation and Model Class Selection

Consider a parameterized FE model class M of a nonlinear structure and let $\underline{\theta}_m \in R^N_{\underline{\theta}}$ be the structural model parameters to be estimated using a set of measured response quantities. In nonlinear structural dynamics, the measured quantities may consist of full response time histories $D = \{\underline{\hat{y}}_k \in R^{N_0}, k = 1, \cdots, N\}$ at N_0 DOF and at different time instants $t = k\Delta t$, where k is the time index and N is the number of sampled data with sampling period Δt, or response spectra $D = \{\underline{\hat{y}}_k \in R^{N_0}, k = 1, \cdots, N\}$ at different frequencies ω_k, where $k$is a frequency domain index. In addition, let $\{\underline{y}_k(\underline{\theta}_m) \in R^{N_0}, k = 1, \cdots, N\}$ be the model response predictions (response time histories or response spectra), corresponding to the DOFs where measurements are available, given the model class M and the parameter set $\underline{\theta}_m \in R^{N_\theta}$. It is assumed that the observation data and the model predictions satisfy the prediction error equation

$$\underline{\hat{y}}_k = \underline{y}_k(\underline{\theta}_m|\mathrm{M}_m) + \underline{e}_k \tag{4.1}$$

where the error term $\underline{e}_k \sim N(\underline{\mu}, \Sigma(\underline{\theta}_e))$ is a Gaussian vector with mean zero and covariance $\Sigma(\underline{\theta}_e)$. It is assumed that the error terms $\underline{e}_k$, $k = 1, \cdots, N$ are independent. This assumption may be reasonable for the case where the measured quantities are the response spectra. However, for measured response time histories this assumption is expected to be violated for small sampling periods. The effect of correlation in the prediction error models is not considered in this study. The notation $\Sigma(\underline{\theta}_e)$ is used to denote that a model is postulated for the prediction error covariance matrix that depends on the parameter set $\underline{\theta}_e$.

Bayesian methods are used to quantify the uncertainty in the model parameters as well as select the most probable FE model class among a family of competitive model classes based on the measured data. The structural model class M is augmented to include the prediction error model class that postulates zero-mean Gaussian models. As a result, the parameter set is augmented to include the prediction error parameters $\underline{\theta}_e$. Using PDFs to quantify uncertainty and following the Bayesian formulation (e.g. [2, 3, 11]), the posterior PDF $p(\underline{\theta}|D, \mathrm{M})$ of the structural model and the prediction error parameters $\underline{\theta} = (\underline{\theta}_m, \underline{\theta}_e)$ given the data D and the model class M can be obtained in the form

$$p(\underline{\theta}|D,\mathrm{M}) = \frac{[p(D|\mathrm{M})]^{-1}}{(2\pi \det \Sigma(\underline{\theta}_e))^{NN_0/2}} \exp\left[-\frac{1}{2}J(\underline{\theta})\right] \pi(\underline{\theta}|\mathrm{M}) \tag{4.2}$$

where

$$J(\theta) = \sum_{r=1}^{m} [\underline{y}(\underline{\theta}_m) - \underline{\hat{y}}]^T \Sigma^{-1}(\underline{\theta}_e)[\underline{y}(\underline{\theta}_m) - \underline{\hat{y}}]^T \tag{4.3}$$

is the weighted measure of fit between the measured and model predicted quantities, $\pi(\underline{\theta}|\mathrm{M})$ is the prior PDF of the model parameters $\underline{\theta}$ and $p(D|\mathrm{M})$ is the evidence of the model class M.

For a large enough number of experimental data, and assuming for simplicity a single dominant most probable model, the posterior distribution of the model parameters can be asymptotically approximated by the multi-dimensional Gaussian distribution [2, 11] centered at the most probable value $\underline{\hat{\theta}}$ of the model parameters that minimizes the function $g(\underline{\theta};\mathrm{M}) = -\ln p(\underline{\theta}|D,\mathrm{M})$ with covariance equal to the inverse of the Hessian $h(\underline{\theta})$ of the function $g(\underline{\theta};\mathrm{M})$ evaluated at the most probable value. For a uniform prior distribution, the most probable value of the FE model parameters $\underline{\theta}$ coincides with the estimate obtained by minimizing the weighted residuals in (4.3). An asymptotic approximation based on Laplace's method is also available to give an estimate of the model evidence $p(D|\mathrm{M})$ [11]. The estimate is also based on the most probable value of the model parameters and the value of the Hessian $h(\underline{\theta})$ evaluated at the most probable value.

The Bayesian probabilistic framework is also used to compare two or more competing model classes and select the optimal model class based on the available data. Consider a family $\mathrm{M} = \{\mathrm{M}_i,\, i = 1,\cdots,\mu\}$, of μ alternative, competing, parameterized FE and prediction error model classes and let $\underline{\theta}_i \in R^{N_{\theta_i}}$ be the free parameters of the model class M_i. The posterior probabilities $P(\mathrm{M}_i|D)$ of the various model classes given the data D is [4]

$$P(\mathrm{M}_i|D) = \frac{p(D|\mathrm{M}_i)P(\mathrm{M}_i)}{p(D|\mathrm{M}_{Fam})} \tag{4.4}$$

where $P(\mathrm{M}_i)$ is the prior probability and $p(D|\mathrm{M}_i)$ is the evidence of the model class M_i. The optimal model class M_{best} is selected as the one that maximizes $P(M_i|D)$ given by (4.4). For the case where no prior information is available, the prior probabilities are assumed to be $P(M_i) = 1/\mu$, so the model class selection is based solely on the evidence values.

The asymptotic approximations may fail to give a good representation of the posterior PDF in the case of multimodal distributions or for unidentifiable cases manifested for relatively large number of model parameters in relation to the information contained in the data. For more accurate estimates, one should use SSA to generate samples that populate the posterior PDF in (4.2). Among the SSA available, the TMCMC algorithm [7] is one of the most promising algorithms for selecting the most probable model class among competitive ones, as well as finding and populating with samples the importance region of interest of the posterior PDF, even in the unidentifiable cases and multi-modal posterior probability distributions. In addition, the TMCMC samples $\underline{\theta}^{(i)}$, $i = 1,\cdots,N_s$ drawn from the posterior distribution can be used to yield an estimate of the evidence $p(D|\mathrm{M}_i)$ required for model class selection [7, 12, 13]. The TMCMC samples can further be used for estimating the probability integrals encountered in robust prediction of various performance quantities of interest [6]. In particular, if $q(\underline{\theta})$ is an output quantity of interest conditional on the value of the parameter set $\underline{\theta}$, the posterior robust measure of q given the data and taking into account the uncertainty in $\underline{\theta}$ is obtained from the sample estimate

$$E(q|D,\mathrm{M}) = \frac{1}{N_s}\sum_{i=1}^{N} \mu_q(\underline{\theta}^{(i)};\mathrm{M}) \tag{4.5}$$

where $\mu_q(\underline{\theta}^{(i)};\mathrm{M})$ is the conditional mean value of $q(\underline{\theta})$ given the model class.

4.3 Application to a Small Scale Laboratory Vehicle Model

In order to simulate the response of a ground vehicle an experimental device was selected and set up [14]. More specifically, the selected frame structure comprises a frame substructure with predominantly linear response and high modal density plus four supporting substructures with strongly nonlinear action. First, Fig. 4.1a shows a picture with an overview of the experimental set up. In particular, the mechanical system tested consists of a frame substructure (parts with red, gray and black color), simulating the frame of a vehicle, supported on four identical substructures. These supporting substructures consist of a lower set of discrete spring and damper units, connected to a concentrated (yellow color) mass, simulating the

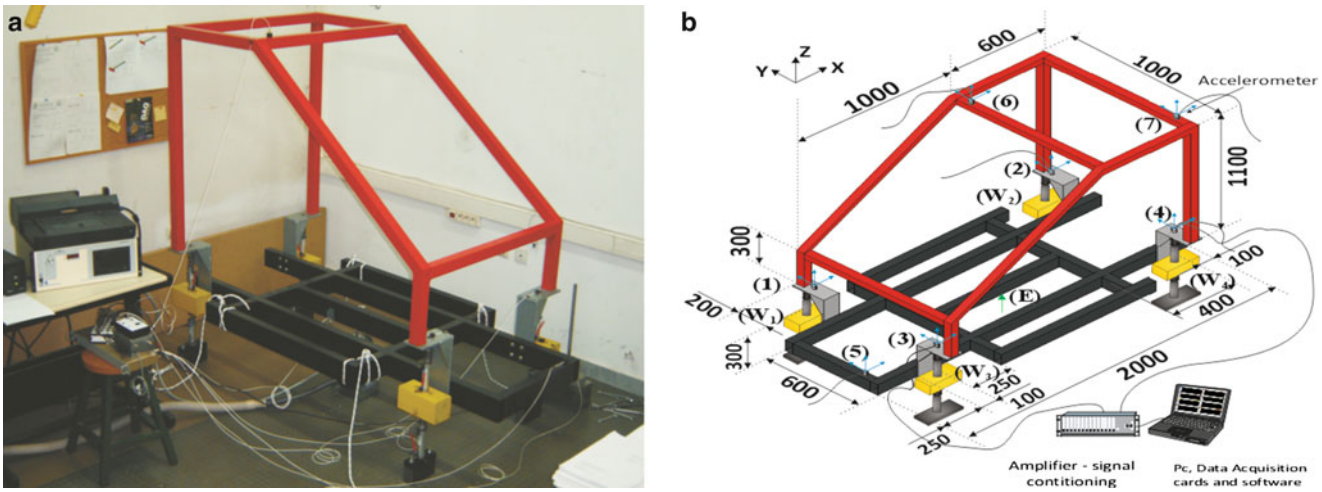

Fig. 4.1 (**a**) Experimental set up of the structure tested, (**b**) dimensions of the frame substructure and measurement points

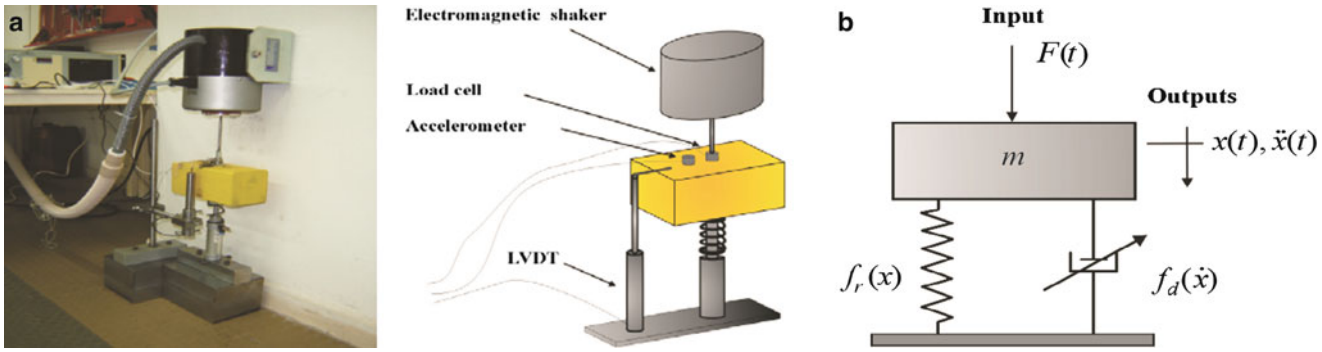

Fig. 4.2 (**a**) Experimental set up for measuring the support stiffness and damping parameters, (**b**) equivalent model

wheel subsystems, as well as of an upper set of a discrete spring and damper units connected to the frame and simulating the action of the vehicle suspension. Also, Fig. 4.1b presents more details and the geometrical dimensions of the frame subsystem. Moreover, the measurement points indicated by 1–4 correspond to connection points between the frame and its supporting structures, while the other measurement points shown coincide with characteristic points of the frame. Finally, point E denotes the point where the electromagnetic shaker is applied.

In order to identify the parameters of the four supporting subsystems, which exhibit strongly nonlinear characteristics, a series of tests was performed. To investigate this further, the elements of the supporting units were disassembled and tested separately. First, Fig. 4.2a shows a picture of the experimental setup and presents graphically the necessary details of the experimental device that was set up for measuring the stiffness and damping properties of the supports, while Fig. 4.2b shows the equivalent mechanical model.

The experimental process was applied separately to both the lower and the upper spring and damper units of the supporting substructures and can be briefly described as follows. First, the system shown in Fig. 4.2 is excited by harmonic forcing through the electromagnetic shaker up until it reaches a periodic steady state response. When this happens, both the history of the acceleration and the forcing signals are recorded at each forcing frequency. Some characteristic results obtained in this manner are presented in the following sequence of graphs. Next, Fig. 4.3a presents the transmissibility function of the system tested, obtained experimentally for three different forcing levels. Specifically, this function is defined as the ratio of the root mean square value of the acceleration to the root mean square value of the forcing signal measured at each forcing frequency. The continuous, dashed and dotted lines correspond to the smallest, intermediate and largest forcing amplitude, respectively. Clearly, the deviations observed between the forcing levels indicate that the system examined possesses nonlinear properties. Moreover, neither the applied forcing is harmonic, especially within the frequency range below $\omega = 10\,\text{Hz}$. To illustrate this, Fig. 4.3b shows two periods of the actual excitation force applied for the same three excitation levels in obtaining the results of Fig. 4.3a, which were recorder at a fundamental forcing frequency of $\omega = 4\,\text{Hz}$.

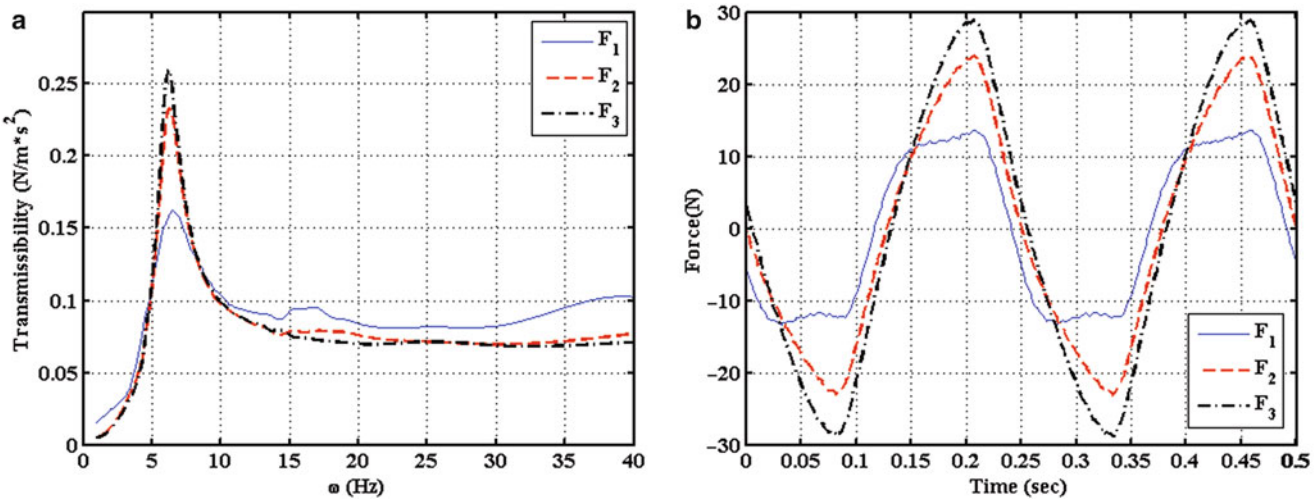

Fig. 4.3 (**a**) Transmissibility function of the support system, for three different forcing levels, (**b**) history of the external force applied with a fundamental harmonic frequency $\omega = 4\,\text{Hz}$

A number of models of the restoring and damping forces, say f_r and f_d, respectively, were tried for modeling the action of the supports and compared with the experimental results. The classic linear dependence of the restoring force on the displacement and of the damping forces on the velocity of the support unit was first assumed. However, critical comparison with the experimental results using the Bayesian model selection framework demonstrated that the outcome was unacceptable in terms of accuracy. Eventually it was found that an acceptable form of the restoring forces is the one where they remain virtually in a linear relation with the extension of the spring, namely

$$f_r(x) = kx \tag{4.6}$$

while the damping force was best approximated by the following formula

$$f_d(\dot{x}) = c_1\dot{x} + \frac{c_2\dot{x}}{c_3 + |\dot{x}|} \tag{4.7}$$

As usual, the linear term in the last expression is related to internal friction at the support, while the nonlinear part is related to the existence and activation of dry friction. More specifically, in the limit $c_3 \to 0$, the second term in the right hand side of Eq. (4.7) represents energy dissipation action corresponding to dry friction. On the other side, in the limit $c_3 \to \infty$, this term represents classical viscous action and can actually be absorbed in the first term.

4.4 Results

The value of the parameters appearing in the assumed models of the restoring and damping forces of the supports, like the coefficients k, c_1, c_2 and c_3 in Eqs. (4.6) and (4.7), are determined by applying the Bayesian uncertainty quantification and calibration methodology. Results are obtained based on experimental response spectra values for both the displacement and acceleration of either the wheel or the suspension component. It is assumed that the prediction errors in the Bayesian formulation are uncorrelated with prediction error variance $\Sigma = diag(\Sigma_1, \Sigma_2) = diag(\sigma_1^2 I, \sigma_2^2 I)$, where $\Sigma_1 = \sigma_1^2 I$ and $\Sigma_2 = \sigma_2^2 I$ are the covariance matrices for the prediction errors corresponding to the displacements and accelerations, respectively. The parameter space is six dimensional and includes $\theta = (k, c_1, c_2, c_3, \sigma_1, \sigma_2)$. Parameter estimation results are obtained using the parallelized and surrogate-based version [10] of the TMCMC algorithm [7] with 500 samples per stage. Eight computer workers were used to perform in parallel the computations involved in the TMCMC algorithm. The computational time required to run all 5,500 samples for the 11 TMCMC stages, without surrogate approximation, for the SDOF model is approximately 7 h. Surrogate modeling [10] reduces further this time by approximately one order of magnitude. For illustration purposes, results for the TMCMC samples projected in the two-dimensional parameter spaces (k_1, c_1) and (c_1, c_2)

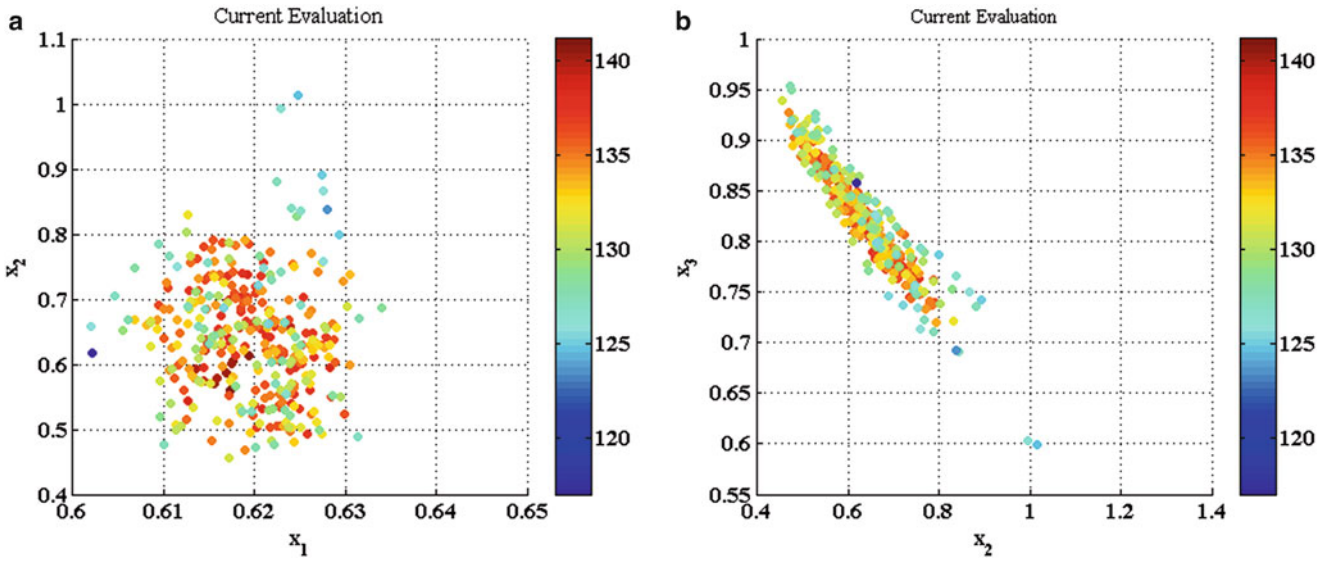

Fig. 4.4 Model parameter uncertainty: projection of TMCMC samples in the two dimensional parameter spaces

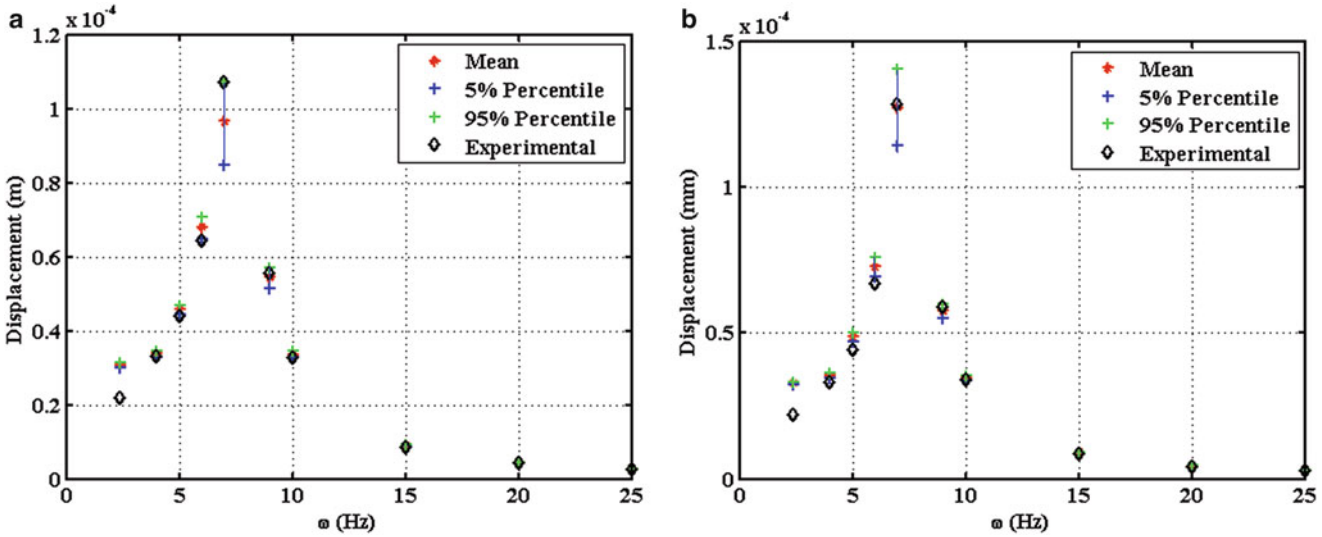

Fig. 4.5 Uncertainty propagation: displacement response spectra uncertainty along with comparisons with the experimental data for the suspension component. (**a**) Moderate excitation level, (**b**) strong excitation level

are shown in Fig. 4.4 for the SDOF system, shown in Fig. 4.2b, corresponding to the suspension component. It is clear that the uncertainties in the damping parameters c_1 and c_2 are relatively high and c_1 and c_2 are highly correlated along certain directions in the parameter space.

The parameter uncertainties are propagated through the SDOF model to estimate the uncertainties in the displacement and acceleration response spectra. The results are shown in Figs. 4.5 and 4.6 for the displacement and acceleration response spectra, respectively and are compared to the experimental values of the response spectra. An adequate fit is observed. Discrepancies between the model predictions and the experimental measurements are mainly due to the model errors related to the selection of the particular forms of the restoring force curves in (4.6) and (4.7). The Bayesian model selection strategy based on Eq. (4.5) can be used to select among alternative restoring force models in an effort to improve the observed fit.

The above procedure has been repeated for the wheel component to identify the uncertainties in the linear stiffness and nonlinear damping model. In addition, the uncertainties in nine stiffness-related parameters of the frame component were also estimated using the Bayesian methodology and the experimental values the first ten modal frequencies and the mode shape components at 72 locations of the frame [15]. The linear finite element model has 45,564 DOFs. Due to excessive computational cost arising in stochastic simulation algorithms, the model was reduced using a recently developed CMS

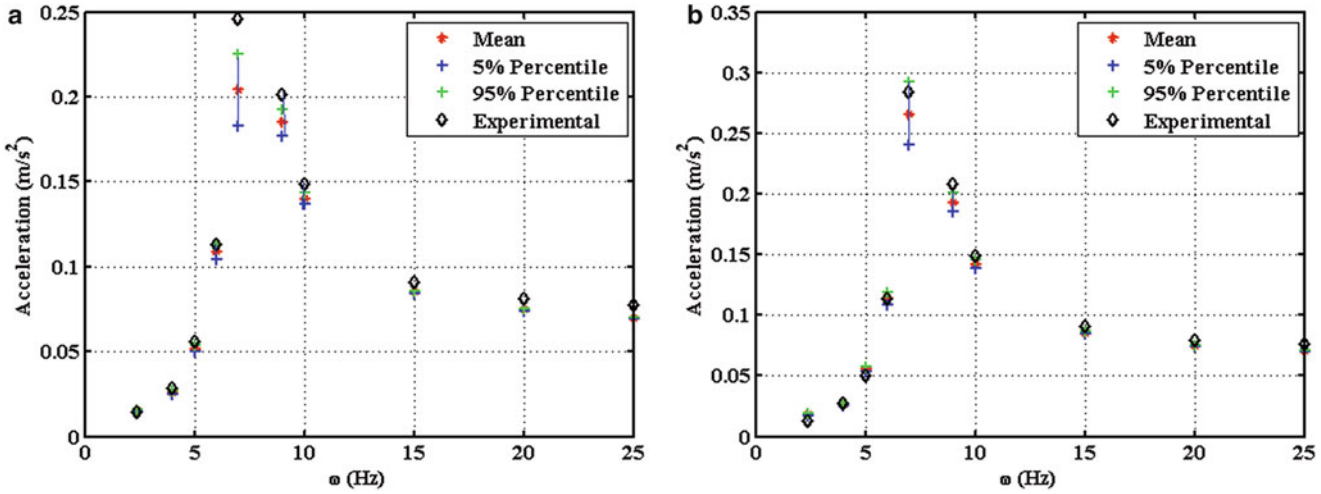

Fig. 4.6 Uncertainty propagation: acceleration response spectra uncertainty along with comparisons with the experimental data for the suspension component. (**a**) Moderate excitation level, (**b**) strong excitation level

method for FE model updating [8]. The reduced model has 30 DOFs, resulting in substantial computational savings of more than two orders of magnitude. Due to space limitations, results of the parameter estimation are not shown here.

The estimates of the model parameter values and their uncertainties for each component are used to build the model for the combined wheel-suspension-frame structure. The number of DOFs of the nonlinear model of the combined structure is 45,568. The parametric uncertainties are then propagated to uncertainties in the response of the combined structure. The CMS was again used to reduce the number of DOFs to 34 and thus drastically reduce the computational effort that arises from the re-analyses due to the large number of TMCMC samples and the nonlinearity of the combined system. Selected uncertainty propagation results are next presented. Specifically, the parameters of the wheel model and the model of the frame structure are kept to their mean values and only the uncertainties in the model parameters of the suspension components are considered. Such uncertainties are propagated to uncertainties for the acceleration transmissibility function at a point on the wheel, the connection of the wheel with the frame and an internal point on the frame as shown in Fig. 4.7. It is observed that a large uncertainty in the response spectra is obtained at the resonance region close to 3.4 Hz, which is dominated by local wheel body deflections. The response in the resonance regions close to 58 and 68 Hz is mainly dominated by deflection of the frame structure. It is observed that the uncertainties in the suspension parameters do not significantly affect the response spectra at the resonance regions. As a result, response spectra obtained experimentally in these resonance regions for the complete vehicle model are not expected to be adequate to identify uncertainties in the parameters of the suspension model.

4.5 Conclusions

A Bayesian UQ&P framework was presented for identifying nonlinear models of dynamic systems using vibration measurements of their components. The use of Bayesian tools, such as stochastic simulation algorithms (e.g., TMCMC algorithm), may often result in excessive computational demands. Drastic reduction in computational effort to manageable levels is achieved using component mode synthesis, surrogate models and parallel computing algorithms. The framework was demonstrated by identifying the linear and nonlinear components of a small-scale laboratory vehicle model using experimental response spectra available separately for each component. Such model uncertainty analyses for each component resulted in building a high fidelity model for the combined system to be used for performing reliable robust response predictions that properly take into account model uncertainties. The theoretical and computational developments in this work can be used to identify and propagate uncertainties in large order nonlinear dynamic systems that consist of a number of linear and nonlinear components.

Acknowledgements This research has been co-financed by the European Union (European Social Fund – ESF) and Greek national funds through the Operational Program "Education and Lifelong Learning" of the National Strategic Reference Framework (NSRF) – Research Funding Program: Heraclitus II. Investing in knowledge society through the European Social Fund.

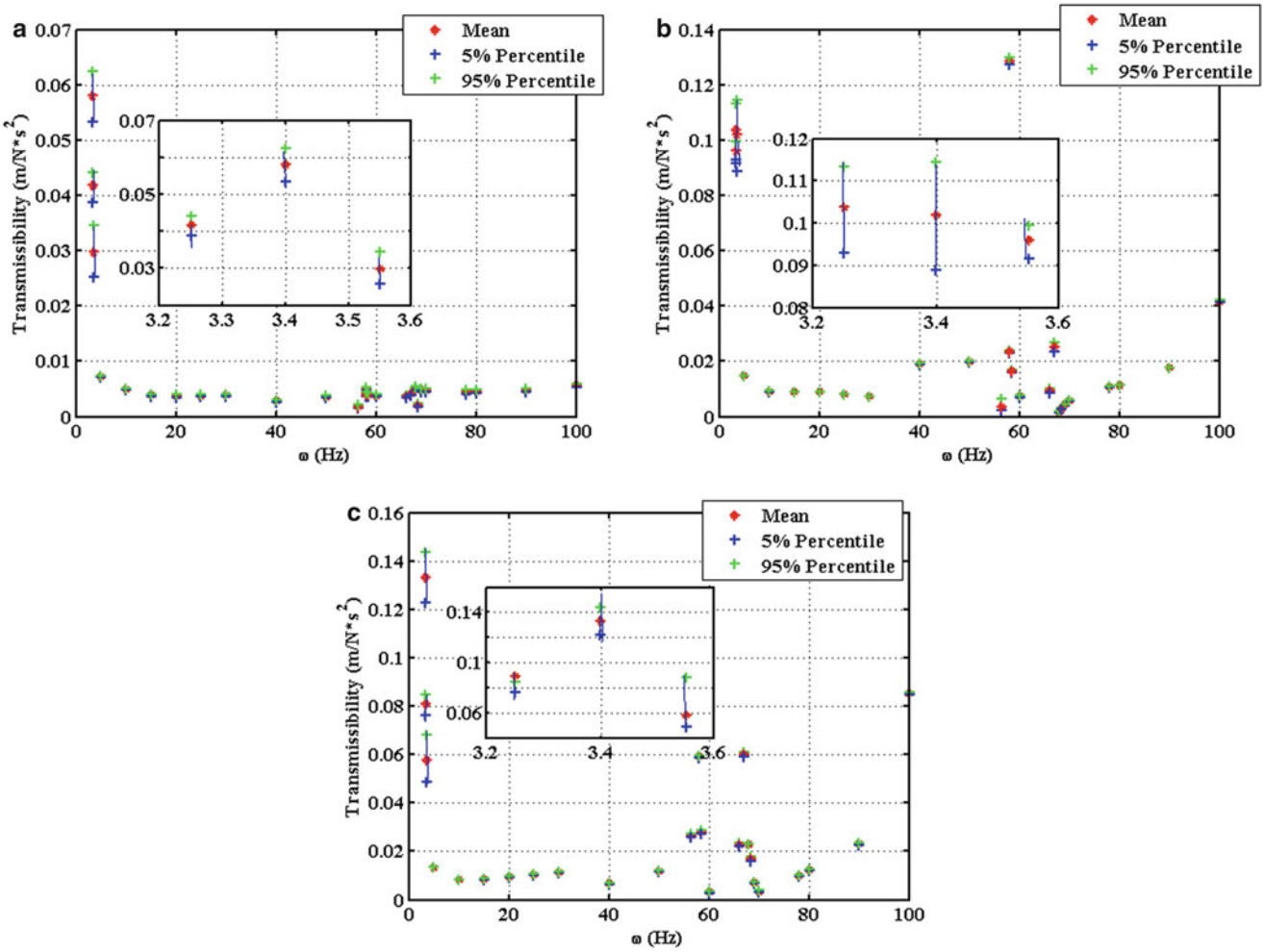

Fig. 4.7 Uncertainty propagation: acceleration transmissibility function uncertainty for combined system. (**a**) Wheel DOF, (**b**) DOF at connection between suspension and frame, (**c**) frame DOF

References

1. Yuen KV, Kuok SC (2011) Bayesian methods for updating dynamic models. Appl Mech Rev 64(1):010802
2. Beck JL, Katafygiotis LS (1998) Updating models and their uncertainties- I: Bayesian statistical framework. ASCE J Eng Mech 124(4):455–461
3. Yuen KV (2010) Bayesian methods for structural dynamics and civil engineering. Wiley, Singapore/Hoboken
4. Beck JL, Yuen KV (2004) Model selection using response measurements: Bayesian probabilistic approach. ASCE J Eng Mech 130(2):192–203
5. Yuen KV (2010) Recent developments of Bayesian model class selection and applications in civil engineering. Struct Saf 32(5):338–346
6. Papadimitriou C, Beck JL, Katafygiotis LS (2001) Updating robust reliability using structural test data. Probab Eng Mech 16:103–113
7. Ching J, Chen YC (2007) Transitional Markov Chain Monte Carlo method for Bayesian updating, model class selection, and model averaging. ASCE J Eng Mech 133:816–832
8. Papadimitriou C, Papadioti DC (2012) Component mode synthesis techniques for finite element model updating. Comput Struct. doi:10.1016/j.compstruc.2012.10.018
9. Papalukopoulos C, Natsiavas S (2007) Dynamics of large scale mechanical models using multi-level substructuring. ASME J Comput Nonlinear Dyn 2:40–51
10. Angelikopoulos P, Papadimitriou C, Koumoutsakos P (2012) Bayesian uncertainty quantification and propagation in molecular dynamics simulations: a high performance computing framework. J Chem Phys 137(14). doi:10.1063/1.4757266
11. Christodoulou K, Papadimitriou C (2007) Structural identification based on optimally weighted modal residuals. Mech Syst Signal Process 21:4–23
12. Muto M, Beck JL (2008) Bayesian updating and model class selection using stochastic simulation J Vib Control 14:7–34

13. Beck JL, Au SK (2002) Bayesian updating of structural models and reliability using Markov chain Monte Carlo simulation. ASCE J Eng Mech 128(4):380–391
14. Giagopoulos D, Natsiavas S (2007) Hybrid (numerical-experimental) modeling of complex structures with linear and nonlinear components. Nonlinear Dyn 47:193–217
15. Papadimitriou C, Ntotsios E, Giagopoulos D, Natsiavas S (2011) Variability of updated finite element models and their predictions consistent with vibration measurements. Struct Control Health Monit. doi:10.1002/stc.453